Qualitative and Quantitative Analyses of Protein Phosphorylation in Naive and Stimulated Mouse Synaptosomal Preparations*[S]

Richard P. Munton‡§, Ry Tweedie-Cullen‡§, Magdalena Livingstone-Zatchej‡§, Franziska Weinandy‡, Marc Waidelich‡, Davide Longo‡, Peter Gehrig¶, Frank Potthast¶, Dorothea Rutishauser¶, Bertran Gerrits¶, Christian Panse¶, Ralph Schlapbach¶, and Isabelle M. Mansuy‡‖

Activity-dependent protein phosphorylation is a highly dynamic yet tightly regulated process essential for cellular signaling. Although recognized as critical for neuronal functions, the extent and stoichiometry of phosphorylation in brain cells remain undetermined. In this study, we resolved activity-dependent changes in phosphorylation stoichiometry at specific sites in distinct subcellular compartments of brain cells. Following highly sensitive phosphopeptide enrichment using immobilized metal affinity chromatography and mass spectrometry, we isolated and identified 974 unique phosphorylation sites on 499 proteins, many of which are novel. To further explore the significance of specific phosphorylation sites, we used isobaric peptide labels and determined the absolute quantity of both phosphorylated and non-phosphorylated peptides of candidate phosphoproteins and estimated phosphorylation stoichiometry. The analyses of phosphorylation dynamics using differentially stimulated synaptic terminal preparations revealed activity-dependent changes in phosphorylation stoichiometry of target proteins. Using this method, we were able to differentiate between distinct isoforms of Ca^{2+}/calmodulin-dependent protein kinase (CaMKII) and identify a novel activity-regulated phosphorylation site on the glutamate receptor subunit GluR1. Together these data illustrate that mass spectrometry-based methods can be used to determine activity-dependent changes in phosphorylation stoichiometry on candidate phosphopeptides following large scale phosphoproteome analysis of brain tissue. ***Molecular & Cellular Proteomics 6:283–293, 2007.***

Activity-dependent protein phosphorylation is one of the most ubiquitous and vital biochemical processes that contributes to the regulation and fine tuning of numerous cellular functions in many cell types. At the molecular level, the addition or removal of a phosphate residue can considerably affect the function and/or localization of proteins including enzymes, ion channels, scaffolding proteins, or signaling molecules. In the nervous system, many proteins are known to be phosphorylated in an activity-dependent fashion in discrete cellular compartments. In synaptic terminals, phosphorylation of pre- and postsynaptic proteins is required for basal neurotransmission and synaptic plasticity at both excitatory and inhibitory connections. Multiple protein kinases and phosphatases are necessary for the induction and maintenance of major forms of synaptic plasticity such as long term potentiation, long term depression, or depotentiation (1) and for cognitive functions (2, 3). For instance, phosphorylation can modulate the activity (autophosphorylation at Thr^{286}) and translocation ($Thr^{305/306}$) of CaMKIIα[1] (4) or channel conductivity (Ser^{831} and Ser^{845} for GluR1) (5). Evidence from functional studies underlines the broad requirement for phosphorylation and the existence of many critical targets in nerve cells. For example, tyrosine phosphorylation is important for NMDA receptor gating, although it is unclear how many of the 25 or more tyrosine residues on the NR2A and NR2B C termini play specific biological roles (6). The identification of such targets and their phosphorylation sites is clearly a prerequisite for a full understanding of the molecular mechanisms of brain functions.

Recent advances in proteomics have allowed large scale analysis of phosphopeptides from proteolytic digests of complex samples (7, 8). However, a major limiting factor in these analyses is the restricted selectivity and coverage of phosphopeptides partly due to inherent unsuitability of standard

From the ‡Brain Research Institute, Medical Faculty of the University of Zürich and Department of Biology of the Swiss Federal Institute of Technology and ¶Functional Genomics Center Zürich, University of Zürich and Swiss Federal Institute of Technology, CH-8057 Zürich, Switzerland

Received, February 6, 2006, and in revised form, November 13, 2006

Published, MCP Papers in Press, November 17, 2006, DOI 10.1074/mcp.M600046-MCP200

[1] The abbreviations used are: CaMKII, Ca^{2+}/calmodulin-dependent protein kinase II; NMDA, *N*-methyl-D-aspartate; SCX, strong cation exchange chromatography; PSD, postsynaptic density; iTRAQ, isobaric peptide tags for relative and absolute quantification; GO, gene ontology; DAP, disks large-associated protein; PKC, protein kinase C.

peptide separation and detection techniques to short, hydrophilic, and negatively charged peptides. Notwithstanding interesting data were obtained from the combination of ion exchange fractionation of proteolytic digests and IMAC of phosphopeptides (9–11). But although several studies have examined subcellular neural phosphoproteomes (11–16) the dynamics and stoichiometry of protein phosphorylation in the brain remain unstudied.

Here we describe a comprehensive workflow that allows the identification of biologically important phosphorylation sites from large phosphoproteomics datasets in the adult mouse brain. Using a highly sensitive, selective, and reproducible phosphopeptide enrichment method based on strong cation exchange chromatography (SCX) and IMAC, we identified multiple candidate phosphorylation sites in proteolytic digests of synaptic membranes, postsynaptic densities (PSDs), and synaptic vesicles. The use of synthetic peptides and isobaric peptide tags allowed us to determine the relative and absolute abundance of selected phosphopeptides and ultimately estimate activity-dependent changes in phosphorylation stoichiometry in stimulated synaptosomal preparations. The workflow has the potential to rapidly single out phosphorylation sites likely to be regulated by neural activity and adds a new dimension to the analyses of protein phosphorylation in complex tissue such as the brain.

EXPERIMENTAL PROCEDURES

Sample Preparation—Subcellular fractionation of mouse cortex was performed as described previously (17). C57/B6 mice (2–5 months old) were sacrificed by cervical dislocation, and the cortex was rapidly removed and washed in ice-cold Buffer A (0.32 M sucrose, 4 mM HEPES, pH 7.4 with the addition of protease mixture inhibitor tablets (Roche Applied Science) and phosphatase inhibitor mixtures I and II (Sigma)). Cortices were homogenized in 10 volumes of Buffer A by 12–15 up-and-down strokes of the homogenizer. The resulting homogenate was centrifuged at 1000 × *g* for 10 min to remove nuclei and cell debris, and supernatant was collected. The pellet was washed again at 1000 × *g*, and the supernatants S1 were combined. The S1 fraction was centrifuged at 17,000 × *g* to give pellet P2, which was washed to give a crude membrane fraction that contains intact synaptosomes. Synaptosomes were lysed by hypotonic shock in 9 volumes of H_2O before addition of HEPES to 4 mM and a 30-min incubation on ice with shaking and centrifuged at 25,000 × *g* to yield pelleted membranes and supernatant S3. The resulting synaptic membranes were made to 0.32 M sucrose and layered over a 0.8 M sucrose solution and centrifuged for 20 min at 230,000 × *g* to separate synaptic membranes and mitochondria from myelin. The pellet containing synaptic and mitochondrial membranes was resuspended in 0.32 M sucrose and layered over a 1.2 M sucrose solution and centrifuged for 20 min at 230,000 × *g* to pellet synaptic membranes. Synaptic vesicles were prepared by pelleting S3 fractions at 165,000 × *g* for 2 h. Crude PSD fractions were prepared by their insoluble properties in 0.5% Triton X-100. Pelleted fractions were frozen at −80 °C until analysis.

KCl Stimulation of Synaptosomes—Synaptosomes were enriched as described above, resuspended in Krebs-Ringer solution, and incubated for 20 min at 37 °C. Samples were stimulated by the addition of KCl to give 50 mM final concentration and incubated for a further 2 min at 37 °C. The reactions were terminated by the addition of ice-cold buffer containing kinase and phosphatase inhibitors before further enrichment of PSDs and synaptic vesicles as described above.

In-solution Digestion—Synaptic protein fractions (0.8–2 mg for phosphopeptide enrichment; 100 μg for iTRAQ (isobaric tags for relative and absolute quantitation) experiments) were desalted by acetone precipitation. For phosphopeptide enrichment experiments, desalted protein was solubilized in 7 M urea, 100 mM ammonium bicarbonate, pH 8.0; reduced with 12.5 mM DTT for 30–60 min; alkylated with 40 mM iodoacetamide for 1 h; and diluted to 1.5 M urea with 100 mM ammonium bicarbonate. For iTRAQ experiments, samples were solubilized and cysteine-blocked according to the manufacturer's protocols. Samples were digested overnight with trypsin (Promega) at 37 °C (1:50 enzyme:substrate) or endoproteinase Glu-C (PrinSep) at 30 °C (1:50 enzyme:substrate).

Strong Cation Exchange Peptide Fractionation—The peptide-containing solution was acidified to pH <3 with acetic acid, made to 25% acetonitrile, and centrifuged at 16,000 × *g* for 10 min to remove insoluble matter. Peptides were then loaded onto a 4.6 × 200-mm (phosphopeptide experiments) or 2.1 × 200-mm (iTRAQ experiments) PolySULFOETHYL aspartamide A column (PolyLC) on an Agilent HP1100 binary HPLC system. Phosphopeptide-rich fractions were eluted with an increasing KCl gradient (0–105 mM over 30 min and 105–350 mM over the following 20 min) in 10 mM KH_2PO_4, 25% acetonitrile, pH 3. The first five fractions were then lyophilized to remove acetonitrile, desalted with Sep-Pak reverse-phase cartridges (Waters), and lyophilized to 100 μl. For iTRAQ experiments, peptides were eluted in a two-step KCl gradient (0–150 mM over 30 min; 150–500 mM over the following 20 min).

iTRAQ Reagent Labeling and Absolute Quantification—Synthetic peptides (Mimotopes) were designed according to previously observed peptide sequences from MS analysis of synaptic terminal digests and were purified by reverse-phase chromatography. Lyophilized peptides were reconstituted in 1 mM stock solutions. To perform absolute quantification, aliquots containing 20 pmol of a library of peptides were prepared and stored at −80 °C. For relative or absolute quantification experiments, 100 μg of digested synaptic terminal protein or known quantities of synthetic peptides were labeled differentially with iTRAQ reagents according to the manufacturer's instructions and combined before SCX fractionation and LC-MALDI analysis.

Immobilized Metal Affinity Enrichment of Phosphopeptides—Iminodiacetic acid-coupled Sepharose Fast Flow beads were washed with 5 volumes of water, 5 volumes of wash buffer (74:25:1 water:acetonitrile:acetic acid), and 5 volumes of 1 mM $FeCl_3$ before equilibrating in 5 volumes of wash buffer. Peptides from SCX fractionation were loaded onto 75 μl of a 25% bead slurry and incubated at room temperature for 30 min. The samples were carefully washed three times with wash buffer and eluted with 100 mM sodium phosphate buffer, pH 8.9. Samples were concentrated and desalted with ZipTips (Millipore) before lyophilization and stored at −20 °C for analysis by mass spectrometry.

Peptide Separation, Mass Spectrometry, and Database Analysis—Samples were resuspended in 5% acetonitrile, 0.2% formic acid; separated onto a reverse-phase capillary column; and measured directly by nanospray ion trap mass spectrometry. Alternatively the column effluent was directly mixed with MALDI matrix solution (5 mg/ml α-cyano-4-hydroxycinnamic acid in 70% acetonitrile with the addition of 1 mM ammonium citrate) and measured by tandem MALDI-MS.

LC-ESI-MS/MS Analysis Using LCQ Deca—Samples were resuspended in 5% acetonitrile, 0.2% formic acid and loaded onto a reverse-phase capillary column (Magic C_{18}, 75 μm × 8 cm; 200 Å, TipiTips-ED) using a fully automated nanoflow LC system consisting of a PAL autosampler (CTC Analytics AG) and binary Rheos 2000 pump (Flux Instruments). All LC-MS/MS runs of peptides were per-

formed using a 160-min binary gradient using solvents A (5% acetonitrile, 0.2% formic acid) and B (80% acetonitrile, 0.2% formic acid). Peptides were eluted with the following linear gradient: 0–3 min, 0–10% solvent B; 3–50 min, 10–50% solvent B; 50–60 min, 50–100% B followed by 100% B for 5 min and 100% A for 22 min to equilibrate. Average flow at the tip was ~0.25 μl/min after splitting. The LC system was directly coupled to a ThermoFinnigan LCQ Deca ion trap mass spectrometer equipped with a nanospray ionization source. Each MS full scan was followed by three MS/MS spectra of the three most intense peaks. Dynamic exclusion was enabled using the following conditions: repeat count, 2; repeat duration, 1 min; exclusion duration, 4 min; exclusion mass width, 3 Da; and a reject mass list with the following masses: 304.0, 371.0, 391.0, 445.0, 1522.0, 1622.0, 1722.0, and 1822.0.

LC-ESI-MS/MS Analysis of Phosphopeptides Using LTQ-FT—Nano-LC-MS/MS of phosphopeptides was carried out on an Agilent 1100 nano-HPLC system (Agilent Technologies) coupled to an LTQ-ICR-FT (Thermo Electron) mass spectrometer. Peptides were eluted from a home-packed C_{18} tip column with an acetonitrile gradient from 3 to 60% over ~60 min. Mass accuracy (FT and ion trap) were calibrated immediately before the measurements according to the manufacturer's instructions. Up to four data-dependent tandem mass spectra were allowed, measured in the LTQ ion trap. The automatic gain control target settings for the allowed number of ions in the respective mass analyzers were set to $1e^5$ for FT full MS and $1e^4$ for ion trap MS/MS scans. Dynamic exclusion and reject masses were used as described above, corrected for the more accurate mass measurement.

Nanoflow Reverse-phase HPLC Separation and MALDI Spotting—Peptide separation was performed on an Ultimate chromatography system equipped with a Probot MALDI spotting device and Famos autosampler (Dionex-LC Packings). 20 μl of the samples were injected and loaded directly onto a 75-μm × 150-mm separation column (Inertsil ODS-3, 5 μm; Dionex-LC Packings). Peptides were eluted with the following gradient: 0–5 min, 0% solvent B; 5–65 min, 0–50% solvent B; 65–75 min, 50–100% solvent B, and 75–80 min, 100% solvent B. Solvent A contained 0.1% TFA in 98:2 water:acetonitrile, and solvent B contained 0.1% TFA in 20:80 water:acetonitrile, and the flow rate was 300 nl/min. For MALDI-MS/MS analysis, column effluent was directly mixed with MALDI matrix solution (5 mg/ml α-cyano-4-hydroxycinnamic acid in 70% acetonitrile with the addition of 1 mM ammonium citrate) at a flow rate of 1.1 μl/min via a μ-tee fitting. Fractions were automatically deposited every 20 s onto the MALDI target plate (Applied Biosystems) using a Probot microfraction collector. For each HPLC run, a total of 192 spots were collected.

MALDI Mass Spectrometry—MALDI plates were analyzed on a 4700 Proteomics Analyzer MALDI-TOF/TOF system (Applied Biosystems). The instrument was equipped with a Nd:YAG (neodymium-doped yttrium aluminium garnet) laser operating at 200 Hz. The mass spectra were externally calibrated using peptide standards, and spectra from 192 spots per MALDI plate were generated in positive reflector mode by accumulating data from 1500 laser shots and then analyzed using the Peak Picker software supplied with the instrument. Spectral peaks that met the threshold criteria and were not on the exclusion list were included in the acquisition list for the MS/MS spectra. The threshold criteria were set as follows: mass range, 750–4000 Da; minimum signal-to-noise ratio, 40; precursors/spot, 8. Peptide collision-induced dissociation was performed at a collision energy of 1 keV and a collision gas pressure of 2×10^{-7} torr for phosphopeptide enrichment and 5×10^{-7} torr for iTRAQ experiments. During MS/MS data acquisition, a method with a stop condition was used. In this method, a minimum of 3000 shots (60 subspectra accumulated from 50 laser shots each) and a maximum of 7500 shots (150 subspectra) were allowed for each spectrum. The accumulation of additional laser shots was halted whenever at least four ions with a signal-to-noise ratio of at least 50 were present in the accumulated MS/MS spectrum in the region from *m/z* 200 to 90% of the precursor mass.

Data Analysis—MS and MS/MS data were searched using Mascot version 2.1.0 (Matrix Science, London, UK) or Mascot version 1.9.05 (iTRAQ experiments) as the search engine (18). Database searching of MS/MS spectra was performed using a mouse protein database downloaded from the European Bioinformatics Institute (32,849 sequences; 14,519,475 residues; release date, March 25, 2006; source, ftp.ebi.ac.uk/pub/databases/SPproteomes/fasta/proteomes/59.M_musculus.fasta.gz). Modifications used include carbamidomethylation (Cys, fixed; phosphopeptide enrichment experiments), MMTS (Cys, fixed; iTRAQ experiments), oxidation (Met, variable; iTRAQ experiments), pyro-Glu (Gln, variable), *N*-acetyl (protein, variable; MALDI only), and phospho (STY, variable). For ThermoFinnigan LCQ measurements, the average mass of +1, +2, and +3 charge peptides was searched with a peptide tolerance of 1.5 Da and MS/MS tolerance of 0.8 Da. For ThermoFinnigan LTQ-FT measurements, the monoisotopic mass of +1, +2, and +3 charge peptides was searched with a peptide tolerance of 15 ppm and MS/MS tolerance of 0.8 Da. Searches using MALDI-MS/MS spectra were performed for monoisotopic peptides with +1 charge. Error limits were set at 85 ppm for precursor masses and 0.2 Da for fragment ions. For data acquired from the ESI mass spectrometer Mascot generic files were submitted to Mascot search engine using the above described search parameters. For data acquired using the MALDI mass spectrometer, peaks to Mascot software (Applied Biosystems; phosphopeptide enrichment experiments) or GPS (Global Proteome Server) Explorer software (Applied Biosystems; iTRAQ experiments) was used for processing spectra and submitting data for database searching using the search parameters described above. Positive identification of phosphopeptides was performed using a variety of strict criteria including manual inspection of spectra and Mascot expect values of less than 0.05. A normalized delta ion score was calculated for all peptides by taking the difference in the ion score for the top two ranking peptides and dividing that difference by the ion score of the first ranking peptide (19). All phosphopeptides containing more than one serine, threonine, or tyrosine residue and a normalized delta ion score of less than 0.4 (19) were evaluated for precise site assignment. The confirmation of phosphorylation sites was primarily based on the presence of site-specific singly or doubly charged b and y type fragment ions (b and y ions generated by cleavages between two potential phosphorylation sites). Relative intensity of essential diagnostic fragment ions was checked in MS/MS spectra. Rules for increased or decreased peptide cleavage probability were taken into account (enhanced cleavage on N-terminal side of proline and on C-terminal side of aspartic acid and reduced cleavage on C-terminal side of proline). Quantification of iTRAQ reporter ion intensity was performed by integrating the area under reporter ion peaks using Applied Biosystems 4700 Explorer software before combining with database search results. Only peptides with both satisfactory database identification and sufficiently intense iTRAQ reporter ions were selected for subsequent analysis. UniProt accession numbers were processed using GoMiner (20).

RESULTS

Streamlined High Throughput Identification of Phosphorylation Sites—Peptides from proteolytic digests of synaptic membranes, PSD, or synaptic vesicles were first fractionated by charge using SCX and then subjected to a second phosphopeptide-specific enrichment using IMAC. Phosphopeptide-enriched samples were further fractionated by reverse-

phase chromatography and analyzed by LC-MS/MS using either ESI-MS/MS or MALDI-MS/MS. Following the analysis of 17,570 MS/MS spectra, we identified 6743 phosphorylated peptide sequences corresponding to 974 unique phosphorylation sites on 499 proteins (see Supplemental Tables 1 and 2 on line). The specificity of enrichment was extremely high with most samples consisting primarily of phosphopeptides (see Supplemental Fig. 1 on line). Phosphorylation was observed on serine, threonine, and tyrosine residues according to expected ratios (77% Ser, 21% Thr, and 2% Tyr) with a majority of residues being monophosphorylated and 0.4% being diphosphorylated (no tri- or more phosphorylated sites were identified with confidence). Increased coverage of phosphosites was achieved by using complementary proteolytic enzyme endoproteinase Glu-C (instead of trypsin) and other mass spectrometers. In particular, nanoflow LC coupled to MALDI-MS/MS yielded high quality data even though phosphopeptide ionization efficiency is low using this method. In our experiments, the quality and quantity of data from SCX-IMAC workflow were superior to analysis of SCX fractions without phosphopeptide enrichment. Following identification analyses, we investigated the functional significance of collected phosphoproteins and performed hierarchical cluster analysis of annotated gene ontologies from the gene ontology consortium (21). These analyses revealed a high diversity and broad coverage of the collection and provided significant functional representations in different subfractions (Fig. 1, *a* and *b*). In the PSD for instance (Fig. 1*a*), significant representation of gene ontologies included molecular functions (*i.e.* CaMKII activity; GO:0004685; $p = 0.0096$), biological process (*i.e.* regulation of synaptic plasticity; GO:0048167; $p = 0.0242$), or cellular component (*i.e.* extracellular matrix; GO:0031012; $p = 0.0132$). In synaptic vesicles (Fig. 1*b*), significantly represented ontologies were dominated by categories related to microtubule and cytoskeletal proteins, consistent with the large number of sequenced phosphopeptides (italicized in parentheses) for microtubule-associated proteins MAP1A (*25*), MAP1B (*162*), MAP2 (*61*), MAP4 (*13*), or MAPT (Tau) (*45*). Ontologies including molecular function such as synaptic vesicle exocytosis (GO:0016079; $p = 0.0292$) or vesicle-mediated transport (GO:0016192; $p = 0.0306$) were also significantly represented.

Quality control was performed by analysis of synthetic phosphopeptides corresponding to those identified in phosphoproteome dataset acquisition. A comparison between MS/MS spectra of corresponding synthetic phosphopeptides and experimentally observed phosphopeptides from biological samples resulted in a perfect match, strongly supporting the deduced identity (see Supplemental Fig. 2 on line). A large proportion of identified phosphopeptides were novel, and many were revealed on prominent synaptic proteins. For instance, a total of 21 sites were newly identified on glutamate receptor NMDA (NR2), disks large-associated protein (DAP), protein kinase C (PKC), and CaMKII (Table I). Wherever a distinction was possible, identified phosphorylation sites were found in defined or predicted intracellular domains. Together these data demonstrate the efficiency and specificity of the method and the quality of the collected data.

Relative Quantification of Proteins Using Isobaric Peptide Tags—The recent introduction of iTRAQ of proteins in different samples represents a major breakthrough in quantitative proteomics (22). iTRAQ is based on the differential covalent labeling of peptides from proteolytic digests with one of four iTRAQ reagents resulting in the incorporation of 144.1 Da to peptide N termini and lysine residues. Peptides with different tags are indistinguishable by mass but can be differentiated by CID (normally applied during MS peptide sequencing) through release of a reporter ion, each of which has a different mass (114.1, 115.1, 116.1, or 117.1 Da). The analysis of the intensity of reporter ions allows the simultaneous sequencing and quantification of labeled peptides. We first evaluated the effectiveness and reproducibility of iTRAQ labeling on our protein extracts. Sample digestion followed by iTRAQ labeling showed that the method is efficient and reproducible (see Supplemental Fig. 3 on line). iTRAQ labeling was used to examine the reliability of our subcellular fractionation protocol. Digests of synaptic membranes, PSDs, and synaptic vesicles were differentially labeled with three iTRAQ reagents (114, 115, and 116, respectively) and then fractionated by SCX, and the relative abundance of proteins was determined and compared in each preparation. The results revealed that each fraction carried a specific pool of proteins. PSD preparations were enriched 1.5-fold with 49 specific proteins including glutamate receptors, scaffolding proteins, kinases, and transport proteins (see Supplemental Fig. 4a on line). Likewise synaptic vesicle preparations were highly enriched in several classes of vesicular components such as vesicle proteins, proton pumps, and proteins involved in lipid metabolism (see Supplemental Fig. 4b on line). Notably this latter fraction contained a higher proportion of specific proteins when compared with synaptic membranes or PSD preparations. For example, the clathrin-coated vesicle proton pump (ATP6v0a1) identified from the 1460.8-Da peptide ^{39}DLNPDVNVFQR^{49} was enriched by 7-fold in synaptic vesicle preparations (Fig. 2).

FIG. 1. **High throughput identification of phosphorylation sites in synaptic terminals from mouse cortex.** Phosphopeptides from proteolytic digests of synaptic proteins were selectively enriched using SCX and IMAC and then analyzed by LC-MS/MS. *a* and *b*, hierarchical clustering of gene ontology with corresponding proteins significantly enriched in PSD (*a*) and synaptic vesicles (*b*) determined using GoMiner. Clusters of ontologies can be clearly observed for categories relevant to CaMKII and ionotropic glutamate receptor activity in the PSD or cytoskeletal and vesicular transport proteins in synaptic vesicles. The *scale* indicates the number of phosphopeptides identified for each ontology.

TABLE I

Overview of phosphorylated peptide sequences identified on well characterized synaptic proteins

Seven sequences were identified on glutamate receptor NMDA, several of which are not yet annotated in the databases Phosphosite (www.phosphosite.org), Phosphobase (www.cbs.dtu.dk/databases/PhosphoBase/), or Human Protein Reference Database (www.hprd.org); 10 sequences were identified on PKC. Many other characteristic PSD proteins such as CaMKII, PSD-95, or DAP possess multiple uncharacterized sites.

Protein	Accession	Phosphopeptide	Residue	Position
CaMKIIβ	KCC2B_MOUSE	ESSDSTNTTIEDEDAK	Ser[a]	397
CaMKIIβ	KCC2B_MOUSE	NSSAITSPK	Ser	367
CaMKIIβ	KCC2B_MOUSE	QETVECLKK	Thr	287
CaMKIIγ	KCC2G_MOUSE	QETVECLR	Thr	287
CaMKK1	KKCC1_MOUSE	SFGNPFEPQAR	Ser	458
CaMKK1	KKCC1_MOUSE	SMSAPGSLLMK	Ser[a]	475
CaMKK2	KKCC2_MOUSE	SFGNPFEGSR	Ser[a]	495
mAChR2	ACM2_MOUSE	EPVANQDPVSPSLVQGR	Ser	231
mAChR2	ACM2_MOUSE	EPVANQDPVSPSLVQGR	Ser	233
PSD-93	DLG2_MOUSE	AISLEGEPR	Ser	414
PSD-93	DLG2_MOUSE	QPSVTLQR	Ser[a]	406
PSD-95	DLG4_MOUSE	EQLMNSSLGSGTASLR	Ser	415
PSD-95	DLG4_MOUSE	EQLMNSSLGSGTASLR	Ser	418
PSD-95	DLG4_MOUSE	NTYDVVYLK	Tyr	240
DAP-1	DLGP1_MOUSE	SLDSLDPAGLLTSPK	Thr	436
DAP-1	DLGP1_MOUSE	GCSQDDECVSLR	Ser	509
DAP-1	DLGP1_MOUSE	ATQPSLTELTTLK	Ser[a]	389
DAP-1	DLGP1_MOUSE	AVSEVSINR	Ser[a]	421
DAP-1	DLGP1_MOUSE	GCSQDDECVSLR	Ser	516
DAP-2	DLGP2_MOUSE	ADSIEIYIPEAQTR	Ser	1047
DAP-2	DLGP2_MOUSE	SDVETATDSDTESR	Ser[a]	745
NR1	NMDZ1_MOUSE	AITSTLASSFK	Ser	890
NR2A	NMDE1_MOUSE	QDSLNQNPVSQR	Ser[a]	1025
NR2A	NMDE1_MOUSE	GSLIVDMVSDK	Ser[a]	929
NR2A	NMDE1_MOUSE	KMPSIESDV	Ser	1459
NR2A	NMDE1_MOUSE	SPDFNLTGSQSNMLK	Thr[a]	888
NR2B	NMDE2_MOUSE	NMANLSGVNGSPQSALDFIR	Ser[a]	917
NR2B	NMDE2_MOUSE	QHSYDTFVDLQK	Ser	1303
mGluR7	MGR7_MOUSE	TELCENVDPNSPAAK	Ser[a]	900
PP2Bα	PP2BA_MOUSE	ITSFEEAK	Thr[a]	468
PKCα	KPCA_MOUSE	VISPSEDR	Ser[a]	318
PKCβ	KPCB_MOUSE	HPPVLTPPDQEVIR	Thr	640
PKCϵ	KPCE_MOUSE	LAAGAESPQPASGNSPSEDDR	Ser[a]	337
PKCϵ	KPCE_MOUSE	SAPTSPCDQELK	Ser[a]	350
PKCγ	KPCG_MOUSE	TFCGTPDYIAPEIIAYQPYGK	Thr[a]	514
PKCγ	KPCG_MOUSE	MGPSSSPIPSPSPSPTDSK	Ser[a]	322
PKCγ	KPCG_MOUSE	SPTSPVPVPVM	Ser[a]	687
PKCγ	KPCG_MOUSE	TFCGTPDYIAPEIIAYQPYGK	Thr[a]	518
PKCγ	KPCG_MOUSE	MGPSSSPIPSPSPSPTDSK	Ser[a]	330
PKCγ	KPCG_MOUSE	AAPALTPPDR	Thr	655

[a] A total of 21 phosphorylation sites not annotated at the time of analysis were identified.

Relative Quantification of Activity-dependent Changes in Specific Peptides—Evaluating the relative amount and activity-dependent changes of specific peptides in complex samples is an important step in the understanding of biological functions. Efficient measurement of changes in the level of specific peptide sequences can be performed by using inclusion lists that target desired peptide masses. Such an inclusion list can also help resolve subtle sequence differences between isoforms and allow the quantification of these isoforms. Exploiting the multiplexing possibilities of iTRAQ reagents, we labeled peptides from PSD digests in control and KCl-stimulated synaptosome preparations and targeted several peptides including peptides specific for CaMKIIα and CaMKIIβ isoforms for fragmentation. We used the tryptic peptides ^{284}QETVDCLK^{291} and ^{285}QETVECLK^{292} that differ by a single amino acid substitution (Asp → Glu) in position 5 and are selective for autophosphorylated forms of CaMKIIα or CaMKIIβ, respectively (23). Isolated synaptosomes can function as physiologically independent units containing the necessary machinery for a wide range of cellular mechanisms including protein translation and synaptic signaling and therefore can be used reliably to examine activity-dependent pro-

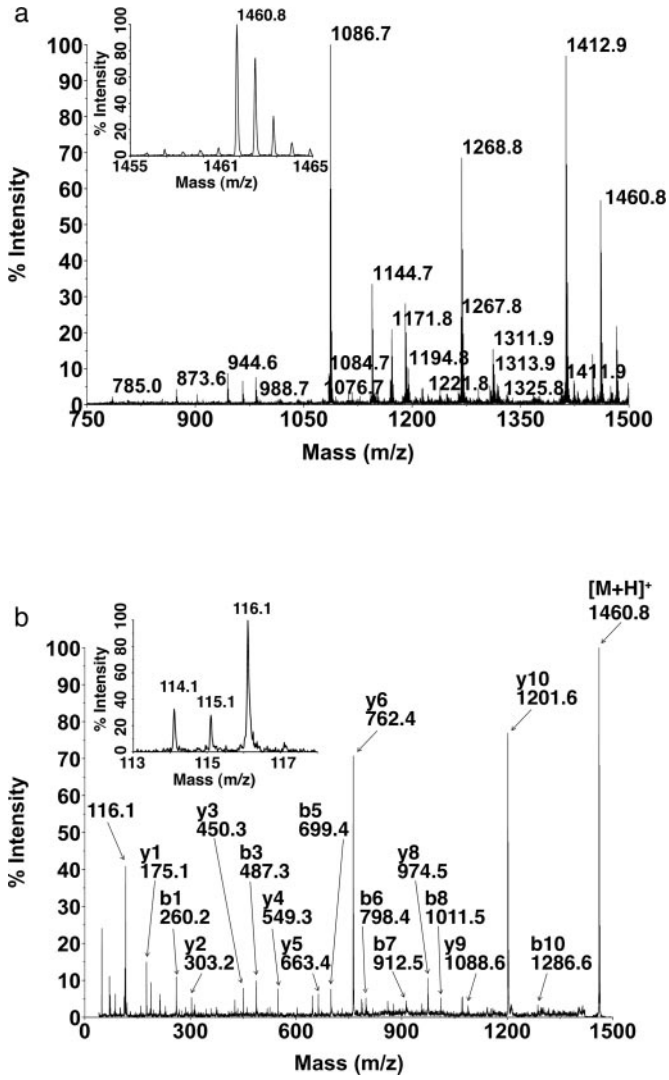

FIG. 2. **Verification of sample preparation purity using isobaric peptide tagging.** Synaptic membranes, PSD, and synaptic vesicles were prepared according to a modified procedure using differential centrifugation before digestion with trypsin. To reduce sample complexity, tryptic peptides were loaded onto an SCX cartridge, and a selected population was eluted with a single 100 mM KCl step. Synaptic membranes, PSDs, and synaptic vesicles were labeled with 114, 115, or 116 iTRAQ reagent, respectively. Labeled peptides were combined and fractionated by charge using SCX before reverse-phase nanoflow separation onto MALDI target plates and analysis by tandem MS. *a*, precursor ion scan for the tryptic peptide ^{39}DLNPDVNVFQR^{49} from ATP6v0a1 at mass 1460.8 Da and close-up (*inset*). *b*, MS/MS scan of ^{39}DLNPDVNVFQR^{49} holding peptide fragmentation information data for sequencing and low mass iTRAQ reporter ion (*inset*) used for relative quantification of synaptic proteins.

cesses (24). Fig. 3*a* shows a precursor ion scan containing both ^{284}QETVDCLK^{291} and ^{285}QETVECLK^{292} peptides *m/z* 1108.6 and 1122.6, and Fig. 3*b* shows the resultant MS/MS for ^{285}QETVECLK^{292} with released iTRAQ reporter ions. Fig. 3*c* shows the quantification of relative changes in the abundance of several specific tryptic CaMKII peptides from different isoforms. Examination of the relative amount of specific peptides relating to phosphorylated and non-phosphorylated sequences reveals changes in phosphoproteins under different experimental conditions. In KCl-stimulated synaptosomes, the amount of phosphorylated CaMKIIα and CaMKIIβ was significantly increased as shown by the increased relative amount of ^{284}QEpTVDCLK^{291} and ^{285}QEpTVECLK^{292} peptides (where pT is phosphothreonine) ($p < 0.05$). Consistently the amount of the corresponding non-phosphorylated peptides ^{284}QETVDCLK^{291} and ^{285}QETVECLK^{292} simultaneously decreased. Additionally examination of isoform-specific peptides ^{434}ITQYLDAGGIPR^{445} and ^{461}FYFENLLAK^{469} indicated no significant change in the total amount of protein. These data illustrate that a careful peptide selection can reveal the behavior of specific modifications on distinct protein isoforms.

Absolute Quantification of Synaptic Phosphoprotein Stoichiometry—An additional major advantage of multiplex iTRAQ labeling is the possibility to determine the molar amount of peptides from sample digests and the amount of protein by including a defined quantity of synthetic peptides labeled with one of the reagents. Initial investigations were conducted to assess the precision of absolute quantification of selected peptides from PSD digests. The results indicated that iTRAQ labeling is precise (less than 7% error) and allowed the determination of the abundance of important synaptic proteins such as CaMKII and glutamate receptors (see Supplemental Fig. 5 on line). We then performed absolute quantification of phosphorylated and non-phosphorylated isoform-specific GluR1 peptides. We labeled corresponding synthetic tryptic peptides with iTRAQ117 and combined them with peptides from stimulated synaptosomes labeled with iTRAQ114–116. Internal standards not only allow the determination of exact molar quantity of peptides in biological samples labeled with iTRAQ114–116 (absolute quantification) but also improve the detection of phosphorylation sites present in low abundance and/or stoichiometry by raising the intensity of ionized peptide ions above the detection threshold. Consequently absolute quantification of both phosphorylated and non-phosphorylated peptides coming from a defined protein can be used to estimate the phosphorylation stoichiometry of a given site. Using this approach, we determined the phosphorylation stoichiometry of several synaptic proteins and found a large range of stoichiometry values (see Supplemental Fig. 6 on line). One phosphopeptide frequently observed in our phosphoproteome screens was ^{691}pSPSAEAAAPPPGPR^{704} (where pS is phosphoserine) from G protein-regulated inducer of neurite outgrowth 1 (Gprin1). Analysis of the ratio of the synthetic phosphopeptide to the amount of phosphorylated (^{691}pSPSAEAAAPPPGPR^{704}) and non-phosphorylated peptide (^{691}SPSAEAAAPPPGPR^{704}) estimated 91% phosphorylation stoichiometry (6.0 pmol phosphorylated and 0.6 pmol non-phosphorylated). Conversely CaMKII and GluR1, known to be phosphorylated during excitatory neuronal signaling,

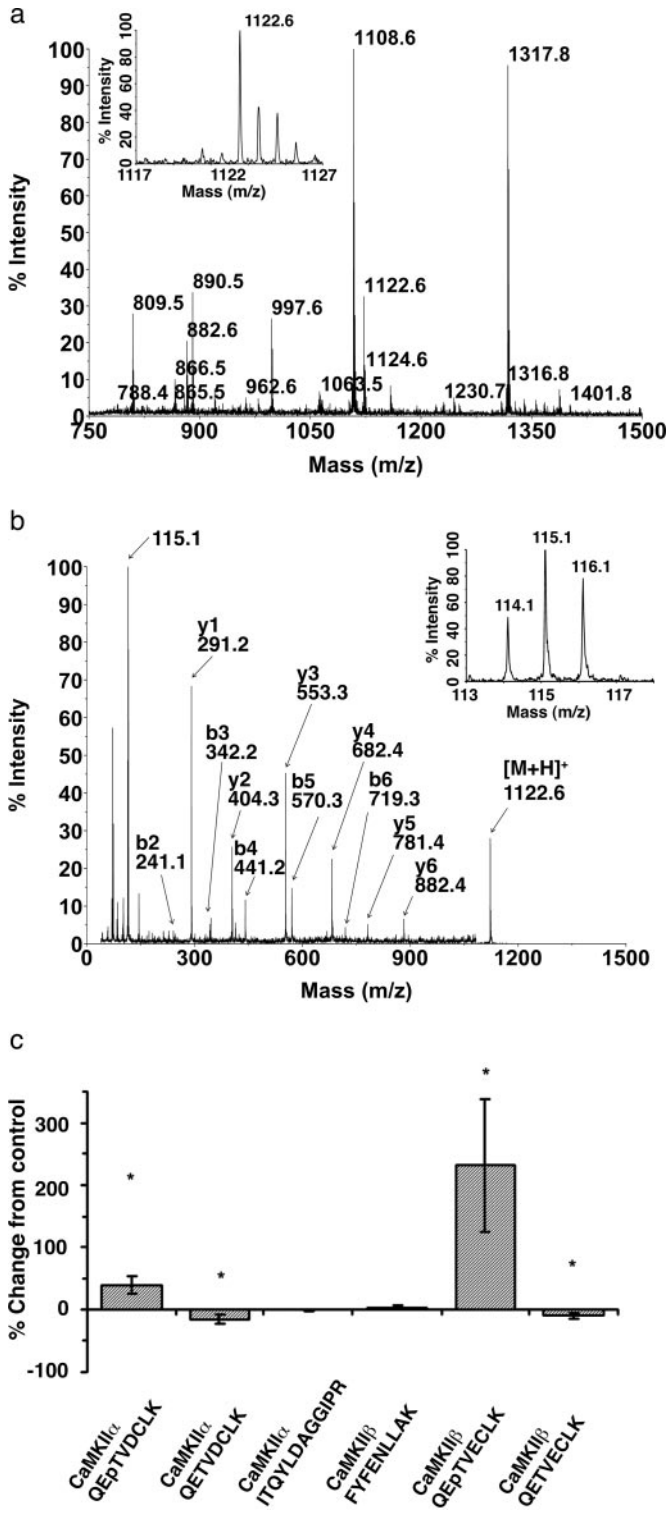

FIG. 3. **Relative quantification of CaMKIIα and CaMKIIβ peptides in PSDs after KCl stimulation.** Tryptic digests were labeled with iTRAQ reagents (KCl-stimulated, iTRAQ114 and -116; control, iTRAQ115) and combined, then fractionated by two-dimensional LC, and analyzed by tandem MS. *a*, precursor ion scan for the tryptic peptide QETVECLK from CaMKIIβ at mass 1122.6 Da and close-up (*inset*). *b*, MS/MS scan of QETVECLK containing peptide fragmentation information data for sequencing and low mass iTRAQ reporter ion (*inset*) used for relative quantification of synaptic proteins. *c*, overview of relative quantification of CaMKII isoform-specific peptide sequences. Following sample standardization, significant increases were observed for the phosphopeptides QEpTVDCLK and QEpTVECLK in KCl-stimulated PSDs ($n = 2$; $p = 0.022$ and 0.023, respectively; *t* test) with no increase for peptides ITQYLDAGGIPR and FYFENLLAK specific to non-phosphorylated regions of CaMKIIα and CaMKIIβ ($n = 2$; $p > 0.1$; *t* test). Consistently a significant decrease in relative amount of non-phosphorylated peptide sequences QETVDCLK and QETVECLK was observed as expected following an increase in phosphorylation of these residues ($n = 2$; *, $p = 0.026$ and 0.022, respectively; *t* test). Data are expressed as mean ± S.E.

had phosphorylation stoichiometry of up to 50%.

To further investigate phosphorylation stoichiometry, we determined the absolute quantity of non-phosphorylated *versus* phosphorylated GluR1 in control and KCl-stimulated conditions. Fig. 4, *a* and *b*, shows the precursor ion and MS/MS scans of the iTRAQ-labeled GluR1 phosphopeptide ^{856}TSpTLPR^{861} at a mass of 898.3 Da. Absolute quantification of ^{856}TSpTLPR^{861} (2.6 pmol/100 μg of PSD) and a corresponding non-phosphorylated GluR1-specific peptide ^{714}YAYLLESTMNEYIEQR^{729} (14 pmol/100 μg of PSD) allowed calculation of basal phosphorylation stoichiometry of 19%. After KCl stimulation, the phosphorylation stoichiometry of GluR1 at Thr^{858} increased to 28% (Fig. 4*c*). Activity-dependent increases in phosphorylation stoichiometry were also observed for CaMKIIα and CaMKIIβ isoforms (Fig. 4*c*). Changes in CaMKIIβ phosphorylation stoichiometry were measured by quantification of the peptides ^{285}QEpTVECLK^{292} and ^{461}FYFENLLAK^{469} for phosphorylated and total CaMKIIβ, respectively, before and after KCl stimulation. Under basal conditions, the peptides were present at 1.4 pmol and 29 pmol/100 μg of PSD, respectively, indicating 5% phosphorylation stoichiometry. After KCl stimulation, this ratio significantly increased to 15%, indicating increased CaMKIIβ phosphorylation with little increase in absolute protein level. A parallel increase in phosphorylation stoichiometry of CaMKIIα isoforms was demonstrated by determining the absolute quantity of the isoform-specific peptides ^{284}QEpTVDCLK^{291} and ^{434}ITQYLDAGGIPR^{445}.

DISCUSSION

A Combined Strategy for the Identification and Absolute and Relative Quantification of Phosphoproteins in Synaptic Terminals—This study describes a workflow to examine activity-dependent changes in phosphorylation level and stoichiometry of candidate sites identified by high throughput post-translational modification analysis on proteins from adult brain. In this multiapproach strategy, each step was optimized to enhance coverage and specificity of phosphoproteomics datasets originating from complex tissue. Optimal protocols were developed for efficient subcellular fractionation of synaptic terminals, sample digestion with complementary pro-

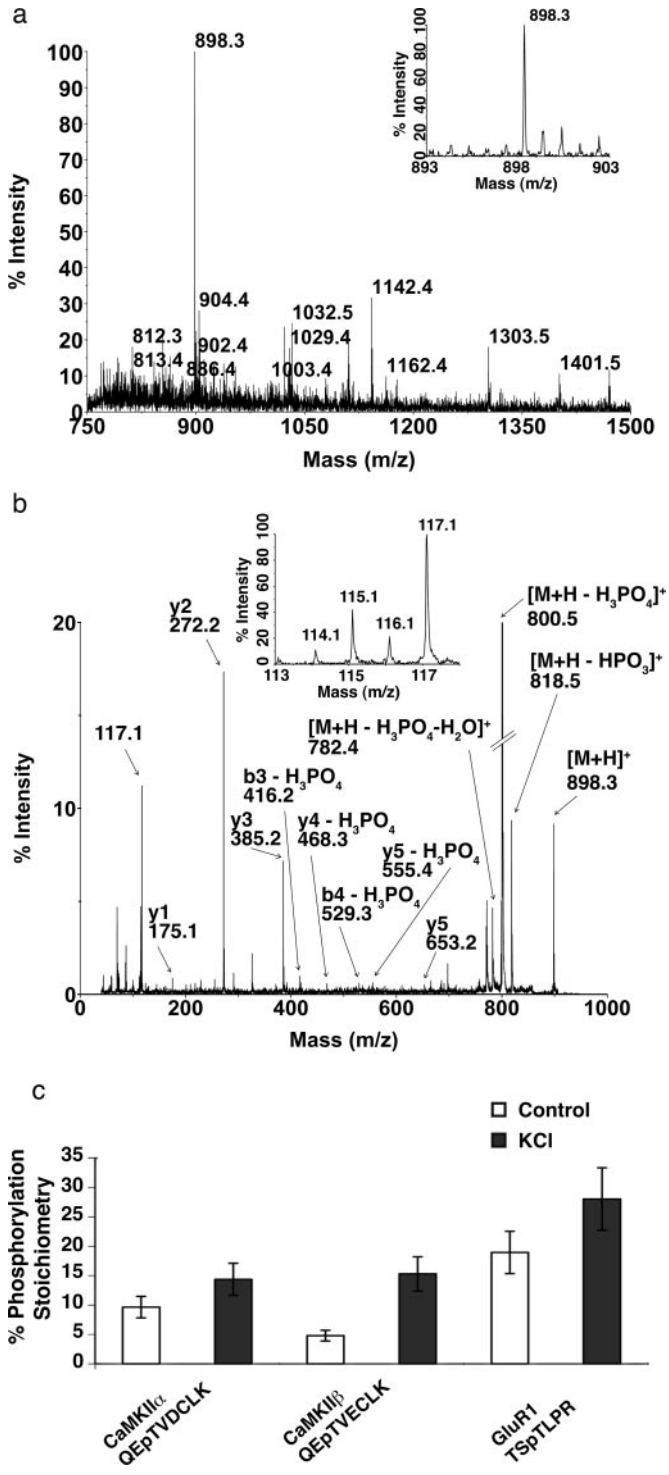

FIG. 4. **Absolute quantification of GluR1-specific phosphorylated and non-phosphorylated peptides in PSDs after KCl stimulation.** Tryptic digests were labeled with iTRAQ reagents (control, iTRAQ114 and -116; KCl-stimulated, iTRAQ115), combined with 20 pmol of iTRAQ117-labeled synthetic peptide, fractionated by two-dimensional LC, and analyzed by tandem MS. *a*, precursor ion scan for the tryptic peptide TSpTLPR from GluR1 at mass 898.3 Da and close-up (*inset*). *b*, MS/MS scan of TSpTLPR containing peptide fragmentation information data for sequencing and low mass iTRAQ reporter ion (*inset*) used for relative and absolute quantification. GluR1 Thr^{858} phosphorylation in PSDs from KCl-stimulated synaptosomes was increased by ~50% compared with control samples. The peak area at 117 Da corresponds to 20 pmol of the synthetic peptide. For clarity, the *y axis* of the spectrum has been magnified 5-fold. *c*, activity-dependent increase in phosphorylation stoichiometry for CaMKIIα, CaMKIIβ, and GluR1 from the PSD of stimulated synaptosomes (control, *white boxes*; stimulated synaptosomes, *black boxes*). Absolute quantification of complementary non-phosphorylated and phosphorylated peptides (as shown in Fig. 3*c*) was used to estimate the upper and lower limit of phosphorylation stoichiometry.

teases, purification and enrichment of phosphopeptides, and a range of mass spectrometers was used. One of the key steps was the development of a protocol for phosphopeptide enrichment with high sensitivity and selectivity that allowed the generation of large phosphopeptide datasets. The low abundance of non-phosphorylated peptides in our samples avoided the usual bias during MS/MS fragmentation and considerably increased the quality and reliability of phosphopeptide identification.

The described analysis of the phosphoproteome in different synaptic terminal preparations from the adult mouse brain extends previous proteomics studies in the nervous system. For example, recent proteomics analyses have described proteins and phosphoproteins in synaptosomes from cerebellar neurons and astrocytes or the PSD (11, 14, 25–28). The emphasis of these studies was primarily on the identification of phosphoproteins in basal conditions rather than on the analysis of changes in phosphorylation and their biological significance. Our identification of novel phosphorylation sites on a large number of synaptic proteins and of activity-dependent changes of some sites provides a major step toward a better understanding of protein functions. It also underscores the extent and dynamics of protein phosphorylation in the adult brain and demonstrates that it is possible to generate functional readouts of protein phosphorylation using proteomics methodologies.

Activity-dependent Phosphorylation of Specific Synaptic Proteins—Applying these methodologies to investigate uncharacterized phosphorylation sites provided novel interesting findings about specific phosphoproteins. For instance, the novel phosphorylation site revealed on GluR1 Thr^{858} was found to lie between two well known sites at Ser^{849} and Ser^{863} (referred to as Ser^{831} and Ser^{845} in the literature) known to be important for several forms of synaptic plasticity and in learning and memory (5). The presence of a third, activity-regulated phosphorylation site on the C terminus of GluR1 provides a potential complementary site for the mechanisms of regulation of the receptor. The extent and specificity of functional modulation of GluR1 by phosphorylation is likely to depend on the extent of phosphorylation of each of the sites implying a "phosphorylation code." Other studies have suggested that clusters of post-translational modifications on intracellular re-

gions of membrane proteins have functional significance (29). Such clusters of phosphorylation sites are thought to exist on many synaptic proteins, creating negatively charged pockets important to modulate or maintain specific functions. This was previously demonstrated for the membrane protein stargazin involved in glutamate receptor trafficking. Stargazin was reported to carry multiple phosphorylation sites that alter the electrostatic properties of the protein tail and increase its mobility and recruitment to the PSD (29). The variable level of phosphorylation was postulated to be the result of a graded level of kinase and phosphatase activity. This graded multiplicity could produce further fine tuning of information processing and storage in synapses. Our phosphoproteomics screens reveal many novel phosphorylation sites in close proximity to previously characterized ones, supporting this possibility.

Advantages of Isobaric Peptide Tags for Absolute Quantification—The major advantages and power of this workflow are illustrated by the determination of CaMKII phosphorylation stoichiometry. Excitatory synaptic signaling is known to facilitate CaMKII phosphorylation resulting in the activation of major forms of synaptic plasticity such as long term potentiation and favoring learning and memory processes (4). Two major isoforms of CaMKII, CaMKIIα and CaMKIIβ, exist in mammalian synapses and are both phosphorylated at homologous positions at Thr^{286} and Thr^{287}, respectively. This degree of similarity makes it difficult to discriminate between the two isoforms by classical approaches. However, this was easily achieved using MS-based methods using the fact that corresponding tryptic peptides differ by a single amino acid substitution.

Another advantage of the method is that the inclusion of synthetic peptide spikes increases the limit of detection of phosphopeptides, in particular low abundance phosphopeptides that are difficult to analyze in complex samples without enrichment. It also offers the option to analyze peptides from smaller samples such as subcellular fractions from selected brain regions. The simultaneous analysis of synthetic and biological peptides can also provide an additional useful means to confirm the existence of putative phosphorylation sites from large phosphoproteome screens as database searches alone are often not sufficient to confidently assign both peptide sequence and modification position. Finally multiplex analysis with isobaric iTRAQ reagents allows the analysis of up to four samples and the simultaneous determination of phosphorylation stoichiometry under three different experimental conditions.

Biological Significance of Phosphorylation Stoichiometry—The biological significance of synaptic protein phosphorylation stoichiometry has not been well addressed up to now because most biochemical experiments to date have examined relative but not absolute changes in phosphorylation under different experimental conditions. The present study investigated both relative and absolute changes in phosphorylation stoichiometry of several prominent synaptic proteins under basal conditions and after KCl stimulation. These analyses revealed that phosphorylation stoichiometry varies significantly between phosphosites and proteins. For instance, 5 and 50% of CaMKII and GluR1, respectively, were estimated to be phosphorylated under resting conditions, while about 91% of Gprin1 was estimated to phosphorylated. The precise biological importance of such phosphorylation stoichiometry is not known. Low stoichiometry in basal conditions is likely to provide a larger window for the action of protein kinases and a broader, possibly faster, dynamic range for protein activation or inhibition during cell signaling. High stoichiometry in contrast may allow more stable, less dynamic, and transient functions such as stabilization of quaternary structure at the plasma membrane or maintenance of homeostatic processes. Future experiments based on the methodology described in this study intend to investigate the functions of novel phosphorylation sites. Additional refinement of experimental protocols should allow, for example, the analysis of specific kinases and phosphatases or pathways stimulated by drug application.

Conclusion—Together these data demonstrate that MS-based proteomics techniques can be used to examine functional aspects of protein phosphorylation in complex tissue such as brain. A small screen of selected phosphorylation sites in defined experimental conditions can help identify candidate phosphorylation sites for downstream analysis. As shown with the novel GluR1 phosphorylation site, the identification of sites modulated by activity provides valuable candidates for subsequent studies investigating the function of phosphorylation. Establishing the ratio of phosphorylated to non-phosphorylated peptides in different experimental conditions using absolute quantification should be useful to studies on synaptic signaling using mathematical models based on interaction networks. Such approaches have the potential to further exploit MS-based techniques to produce functional data and broaden the understanding of post-translational protein modifications.

Acknowledgments—We thank the staff of the Functional Genomic Center Zürich for excellent technical support, Bernd Roschitzki for HPLC, Christian Ahrens for bioinformatics, and Bernd Wollscheid and Ruedi Aebersold for help and constructive discussions.

* This work was supported by the University of Zürich, the Swiss Federal Institute of Technology, the Swiss National Science Foundation, the National Center of Competence in Research "Neural Plasticity and Repair," the Roche Research Foundation, Human Frontier Science Program, and the European Molecular Biology Organization Young Investigator Program. The costs of publication of this article were defrayed in part by the payment of page charges. This article must therefore be hereby marked "*advertisement*" in accordance with 18 U.S.C. Section 1734 solely to indicate this fact.

S The on-line version of this article (available at http://www.mcponline.org) contains supplemental material.

§ These authors made equal contributions to this work.

‖ To whom correspondence should be addressed. Tel.: 41-44-635-33-60; Fax: 41-44-635-33-03; E-mail: mansuy@hifo.unizh.ch.

REFERENCES

1. Malenka, R. C., and Nicoll, R. A. (1999) Long-term potentiation—a decade of progress? *Science* **285,** 1870–1874
2. Bozon, B., Kelly, A., Josselyn, S. A., Silva, A. J., Davis, S., and Laroche, S. (2003) MAPK, CREB and zif268 are all required for the consolidation of recognition memory. *Philos. Trans. R. Soc. Lond. B Biol. Sci.* **358,** 805–814
3. Castellani, G. C., Quinlan, E. M., Bersani, F., Cooper, L. N., and Shouval, H. Z. (2005) A model of bidirectional synaptic plasticity: from signaling network to channel conductance. *Learn. Mem.* **12,** 423–432
4. Lisman, J., Schulman, H., and Cline, H. (2002) The molecular basis of CaMKII function in synaptic and behavioural memory. *Nat. Rev. Neurosci.* **3,** 175–190
5. Lee, H. K., Takamiya, K., Han, J. S., Man, H., Kim, C. H., Rumbaugh, G., Yu, S., Ding, L., He, C., Petralia, R. S., Wenthold, R. J., Gallagher, M., and Huganir, R. L. (2003) Phosphorylation of the AMPA receptor GluR1 subunit is required for synaptic plasticity and retention of spatial memory. *Cell* **112,** 631–643
6. Salter, M. W., and Kalia, L. V. (2004) Src kinases: a hub for NMDA receptor regulation. *Nat. Rev. Neurosci.* **5,** 317–328
7. Peters, E. C., Brock, A., and Ficarro, S. B. (2004) Exploring the phosphoproteome with mass spectrometry. *Mini Rev. Med. Chem.* **4,** 313–324
8. Nesvizhskii, A. I., and Aebersold, R. (2005) Interpretation of shotgun proteomic data: the protein inference problem. *Mol. Cell. Proteomics* **4,** 1419–1440
9. Gruhler, A., Olsen, J. V., Mohammed, S., Mortensen, P., Faergeman, N. J., Mann, M., and Jensen, O. N. (2005) Quantitative phosphoproteomics applied to the yeast pheromone signaling pathway. *Mol. Cell. Proteomics* **4,** 310–327
10. Nuhse, T. S., Stensballe, A., Jensen, O. N., and Peck, S. C. (2003) Large-scale analysis of in vivo phosphorylated membrane proteins by immobilized metal ion affinity chromatography and mass spectrometry. *Mol. Cell. Proteomics* **2,** 1234–1243
11. Trinidad, J. C., Specht, C. G., Thalhammer, A., Schoepfer, R., and Burlingame, A. L. (2006) Comprehensive identification of phosphorylation sites in postsynaptic density preparations. *Mol. Cell. Proteomics* **5,** 914–922
12. Trinidad, J. C., Thalhammer, A., Specht, C. G., Schoepfer, R., and Burlingame, A. L. (2005) Phosphorylation state of postsynaptic density proteins. *J. Neurochem.* **92,** 1306–1316
13. Farr, C. D., Gafken, P. R., Norbeck, A. D., Doneanu, C. E., Stapels, M. D., Barofsky, D. F., Minami, M., and Saugstad, J. A. (2004) Proteomic analysis of native metabotropic glutamate receptor 5 protein complexes reveals novel molecular constituents. *J. Neurochem.* **91,** 438–450
14. Husi, H., Ward, M. A., Choudhary, J. S., Blackstock, W. P., and Grant, S. G. (2000) Proteomic analysis of NMDA receptor-adhesion protein signaling complexes. *Nat. Neurosci.* **3,** 661–669
15. Li, K., Hornshaw, M. P., van Minnen, J., Smalla, K. H., Gundelfinger, E. D., and Smit, A. B. (2005) Organelle proteomics of rat synaptic proteins: correlation-profiling by isotope-coded affinity tagging in conjunction with liquid chromatography-tandem mass spectrometry to reveal post-synaptic density specific proteins. *J. Proteome Res.* **4,** 725–733
16. Yoshimura, Y., Yamauchi, Y., Shinkawa, T., Taoka, M., Donai, H., Takahashi, N., Isobe, T., and Yamauchi, T. (2004) Molecular constituents of the postsynaptic density fraction revealed by proteomic analysis using multidimensional liquid chromatography-tandem mass spectrometry. *J. Neurochem.* **88,** 759–768
17. Carlin, R. K., Grab, D. J., Cohen, R. S., and Siekevitz, P. (1980) Isolation and characterization of postsynaptic densities from various brain regions: enrichment of different types of postsynaptic densities. *J. Cell Biol.* **86,** 831–845
18. Perkins, D. N., Pappin, D. J., Creasy, D. M., and Cottrell, J. S. (1999) Probability-based protein identification by searching sequence databases using mass spectrometry data. *Electrophoresis* **20,** 3551–3567
19. Beausoleil, S. A., Villen, J., Gerber, S. A., Rush, J., and Gygi, S. P. (2006) A probability-based approach for high-throughput protein phosphorylation analysis and site localization. *Nat. Biotechnol.* **24,** 1285–1292
20. Zeeberg, B. R., Feng, W., Wang, G., Wang, M. D., Fojo, A. T., Sunshine, M., Narasimhan, S., Kane, D. W., Reinhold, W. C., Lababidi, S., Bussey, K. J., Riss, J., Barrett, J. C., and Weinstein, J. N. (2003) GoMiner: a resource for biological interpretation of genomic and proteomic data. *Genome Biol.* **4,** R28
21. Ashburner, M., Ball, C. A., Blake, J. A., Botstein, D., Butler, H., Cherry, J. M., Davis, A. P., Dolinski, K., Dwight, S. S., Eppig, J. T., Harris, M. A., Hill, D. P., Issel-Tarver, L., Kasarskis, A., Lewis, S., Matese, J. C., Richardson, J. E., Ringwald, M., Rubin, G. M., and Sherlock, G. (2000) Gene ontology: tool for the unification of biology. The Gene Ontology Consortium. *Nat. Genet.* **25,** 25–29
22. Choe, L. H., Aggarwal, K., Franck, Z., and Lee, K. H. (2005) A comparison of the consistency of proteome quantitation using two-dimensional electrophoresis and shotgun isobaric tagging in Escherichia coli cells. *Electrophoresis* **26,** 2437–2449
23. Colbran, R. J., and Brown, A. M. (2004) Calcium/calmodulin-dependent protein kinase II and synaptic plasticity. *Curr. Opin. Neurobiol.* **14,** 318–327
24. Bagni, C., Mannucci, L., Dotti, C. G., and Amaldi, F. (2000) Chemical stimulation of synaptosomes modulates alpha-Ca^{2+}/calmodulin-dependent protein kinase II mRNA association to polysomes. *J. Neurosci.* **20,** RC76
25. DeGiorgis, J. A., Jaffe, H., Moreira, J. E., Carlotti, C. G., Jr., Leite, J. P., Pant, H. C., and Dosemeci, A. (2005) Phosphoproteomic analysis of synaptosomes from human cerebral cortex. *J. Proteome Res.* **4,** 306–315
26. Li, K. W., Hornshaw, M. P., Van Der Schors, R. C., Watson, R., Tate, S., Casetta, B., Jimenez, C. R., Gouwenberg, Y., Gundelfinger, E. D., Smalla, K. H., and Smit, A. B. (2004) Proteomics analysis of rat brain postsynaptic density. Implications of the diverse protein functional groups for the integration of synaptic physiology. *J. Biol. Chem.* **279,** 987–1002
27. Witzmann, F. A., Arnold, R. J., Bai, F., Hrncirova, P., Kimpel, M. W., Mechref, Y. S., McBride, W. J., Novotny, M. V., Pedrick, N. M., Ringham, H. N., and Simon, J. R. (2005) A proteomic survey of rat cerebral cortical synaptosomes. *Proteomics* **5,** 2177–2201
28. Yang, J. W., Rodrigo, R., Felipo, V., and Lubec, G. (2005) Proteome analysis of primary neurons and astrocytes from rat cerebellum. *J. Proteome Res.* **4,** 768–788
29. Tomita, S., Stein, V., Stocker, T. J., Nicoll, R. A., and Bredt, D. S. (2005) Bidirectional synaptic plasticity regulated by phosphorylation of stargazin-like TARPs. *Neuron* **45,** 269–277